# Identification of a Potent Heterocyclic Ligand To Somatostatin Receptor Subtype 5 by the Synthesis and Screening of $\beta$-Turn Mimetic Libraries

**Andrew J. Souers,[†] Alex A. Virgilio,[†] Åsa Rosenquist,[†] Wasyl Fenuik,[‡] and Jonathan A. Ellman*,[†]**

*Contribution from the Department of Chemistry, University of California, Berkeley, California 94720, and Glaxo Wellcome Cambridge Chemistry Laboratory, University Chemical Laboratory, Lensfield Road, Cambridge, CB2 1EW, UK*

*Received October 26, 1998*

**Abstract:** Methods for the parallel synthesis of medium-ring heterocyclic $\beta$-turn mimetics (**1**) are described, which enable the rapid preparation of libraries of mimetics for the identification of small molecule ligands to receptors. The generality of this method was first demonstrated by the rapid and high-yielding synthesis of mimetics **1a**−**g** that display a wide range of proteinogenic amino acid side chains. Small molecule heterocyclic mimetics of the medicinally important peptide somatostatin were then identified by the synthesis of a focused library of $\beta$-turn mimetics based upon the crucial Trp-Lys motif found in the turn region of somatostatin. Screening the library against a panel of the five cloned human somatostatin receptors ($hSST_1$−$hSST_5$) resulted in the identification of a potent small molecule ligand (**1h**) with selectivity toward $hSST_5$, as well as potent ligands toward receptor subtypes 1−4. Furthermore, structure−activity relationships were used to establish the importance of each of the three diversity inputs present in compound **1h**. This investigation represents the first successful identification of potent, small molecule ligands through the synthesis and evaluation of a *focused* library of turn mimetics (for one example of a successful screening effort of a nonfocused $\beta$-turn library, see: Souers, A. J.; Virgilio, A. A.; Schürer, S.; Ellman, J. A.; Kogan, T. P.; West, H. E.; Ankener, W.; Vanderslice, P. *Bioorg. Med. Chem. Lett.* **1998**, *8*, 2297−2302). The results of the library screening revealed unexpected stereochemical and functional group preferences, reinforcing the critical importance of synthesizing and evaluating collections of mimetics as opposed to traditional iterative synthesis and evaluation approaches. The ability to prepare libraries of heterocyclic turn mimetics that display three different side-chain inputs with multiple distinct side-chain orientations should enable the rapid identification of small molecule heterocyclic ligands to a large number of receptor targets.

## Introduction

Although peptides play an essential role in wide-ranging biological processes, their use as biological probes and therapeutic agents has been complicated by poor receptor subtype selectivity, poor biostability, or unfavorable absorption properties.[2] The design of high affinity and specific constrained peptidomimetic ligands has therefore been an extremely important endeavor in the fields of medicinal chemistry and molecular recognition. In a successfully *designed* peptidomimetic, the essential amino acid side chains of the corresponding peptide are displayed on an alternative scaffold such that the spatial orientation of the side chains corresponds to the display in the bioactive conformation of the peptide.[3] The design and synthesis of peptidomimetic scaffolds based on the $\beta$-turn structure[4a−c] has received the most attention due to the importance of this secondary structural motif in peptide and protein recognition. However, despite considerable effort, very few bioactive small molecule $\beta$-turn mimetics have been developed. The diversity of $\beta$-turn structures found in peptides and proteins severely complicates the determination of the key side chains and the correct display of those side chains in the peptide's bioactive conformation.[5a,b]

We recently reported a preliminary paper on synthesis methods to prepare mimetics[6] based upon the turn structure whereby three amino acid side chains are displayed on a medium-ring heterocyclic scaffold **1** (Figure 1).

A key feature in the design strategy is the capability of performing rapid, parallel synthesis of multiple derivatives in order to overcome the limitations in defining the exact bioactive conformation of the target peptide.[7a,b] The synthetic sequence enables the incorporation of all of the functionality present in the side chains of the proteinogenic amino acids. In addition, to reflect the diversity of side-chain orientations found in

[†] University of California.

[‡] Glaxo Wellcome Cambridge Chemistry Laboratory.

(1) For one example of a successful screening effort of a nonfocused $\beta$-turn library, see: Souers, A. J; Virgilio, A. A.; Schürer, S.; Ellman, J. A.; Kogan, T. P.; West, H. E.; Ankener, W.; Vanderslice, P. *Bioorg. Med. Chem. Lett.* **1998**, *8*, 2297−2302.

(2) Sawyer, T. K. *Structure-Based Design: Diseases, Targets, Techniques and Developments*; Veerapandian. P., Ed.; Marcel Dekker: New York, 1997; pp 559−634.

(3) Gante, J. *Angew. Chem., Int. Ed. Engl.* **1994**, *33*, 1699−1720.

(4) (a) Ball, J. B., Alewood, P. F. *J. Mol. Recognit.* **1990**, *3*, 55−63. (b) Kahn, M. *Synlett* **1993**, *11*, 821−826. (c) Kitagawa, O.; Vander Velde, D.; Dutta, D.; Morton, M.; Takusagawa, F.; Aube, J. *J. Am. Chem. Soc.* **1995**, *117*, 5169−5178.

(5) (a) Wilmot, C. M.; Thornton, J. M. *J. Mol. Biol*. **1988**, *203*, 221−232. (b) Ball, J. B.; Hughes, R. A.; Alewood, P. F.; Andrews, P. R. *Tetrahedron* **1993**, *17*, 3467−3478.

(6) Virgilio, A. A.; Schürer, S. C.; Ellman, J. A. *Tetrahedron Lett.* **1996**, *37*, 6961−6964.

10.1021/ja983742p CCC: $18.00 
Published on Web 02/20/1999

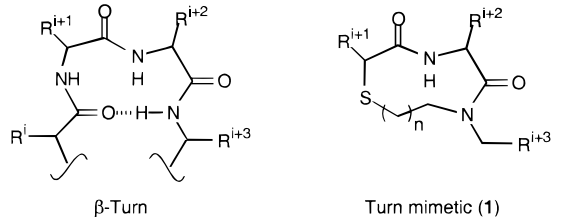


**Figure 1.** Heterocyclic $\beta$-turn mimetic displaying relevant side chains.

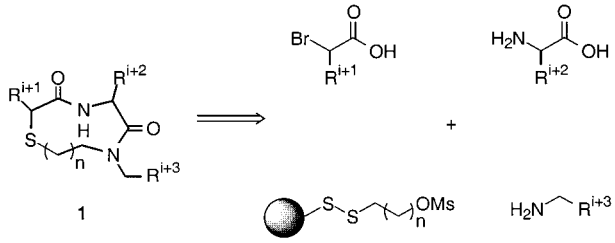


**Figure 2.** The components of the $\beta$-turn mimetic **1**.

proteins, all four possible stereoisomers are accessible at the $i + 1$ and $i + 2$ positions. Side-chain display may also be varied by introducing backbone elements to change the ring size and vectoral display of the amine and thiol functionality. As shown in Figure 2, all of the side-chain precursors are accessed from readily available building blocks: the $i + 3$ side chain is derived from primary amines, the $i + 2$ side chain from Fmoc amino acids, and the $i + 1$ side chain from α-bromo acids, which can be prepared in highly enantioenriched form in a single step from the corresponding side chain protected amino acids.[8]

To establish the ability of heterocycle **1** to serve as a highly effective mimetic of peptide and protein structure, we have focused on the development of potent ligands to the somatostatin receptors. To date, five human somatostatin receptor subtypes ($hSST_1-hSST_5$) have been identified and cloned with each subtype having distinct expression patterns and activities.[9] Somatostatin acts on these receptor subtypes to inhibit the release of a number of pancreatic pituitary and gastrointestinal hormones including glucagon, growth hormone, and insulin. Somatostatin is also present in the nervous system,[10] where it is believed to mediate several processes including cognition and locomoter activity. Due to the wide-ranging biological effects of somatostatin, numerous peptide analogues have been prepared to improve specificity and biostability.[11] These efforts culminated in the development of several potent and specific cyclic peptide analogues with a $\beta$-turn structure as the key binding determinant. These analogues are best exemplified by the cyclic octapeptide octreotide,[12] which is an approved drug for the treatment of carcinomas, acromegaly, and gastro-entero-pancreatic tumors. Unfortunately, octreotide has poor oral bioavailability and must be administered by subcutaneous or intraveneous injection.[13] Clearly, potent small molecule mimetics of somatostatin would be highly desirable.

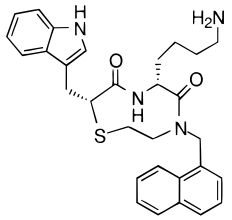


**Figure 3.** Figure 3. A potent nonpeptidal $hSST_5$ ligand.

Peptide ligands to $hSST_5$ inhibit insulin release,[14] and $hSST_5$ has been implicated as the receptor responsible for the antiproliferative effects[15] of somatostatin analogues in normal as well as tumoral cells. Prior design efforts toward small molecule mimetics of somatostatin have produced low micromolar mimetics based upon the display of side chains upon a benzodiazepine scaffold,[16] and through extensive efforts, nonselective high nanomolar ligands based upon the display of side chains upon sugar scaffolds.[17a,b]

Within the past year, Merck[18a,b,c] has identified subnanomolar ligands to the somatostatin receptors and Novo Nordisk[19] has identified low nanomolar ligands to $hSST_4$ by employing massive screening and iterative optimization efforts. Although these screening efforts were ultimately successful, a general strategy for the identification of ligands to receptors through the design, synthesis, and screening of a more focused collection of peptidomimetics has the potential to be considerably more efficient.

Herein, we report for the first time the detailed experimental procedures for the synthesis of $\beta$-turn mimetics **1** and the development of heterocycle **1h** (MW 521) that is a potent small molecule ligand of the $hSST_5$ receptor ($IC_{50} = 87$ nM) (Figure 3).

## Results and Discussion

***β*-Turn Mimetic Synthesis.** The final step in the synthesis of $\beta$ turn mimetic **1** would necessarily be macrocyclization to provide the desired strained medium-ring hetererocycle. Either

(7) (a) Hirschmann and Smith have highlighted the central importance of being able to prepare libraries of peptidomimetics that they have developed based upon sugar scaffolds, but accounts of library synthesis have not been reported. Hirschmann, R.; Hynes, J., Jr.; Cichy-Knight, M. A.; van Rijn, R.; Sprengeler, P.A.; Spoors, P. G.; Shakespeare, W. C.; Pietranico-Cole, S.; Barbosa, J.; Liu, J.; Yao, W.; Rohrer, S.; Smith, A. B., III. *J. Med. Chem.* **1998**, *41*, 1382−1391. (b) Feng, Y.; Wang, Z.; Jin, S.; Burgess, K. *J. Am. Chem. Soc.* **1998**, *121*, 10768−10769.

(8) Souers, A. J.; Schürer, S. C.; Kwack, H. H.; Virgilio, A. A.; Ellman, J. A. *Synthesis* **1998**, in press.

(9) Reisine, T.; Bell, G. I. *Neuroscience* **1995**, *67*, 777−790.

(10) Patel, Y. C. *J. Endocrinol. Invest.* **1997**, *20*, 348−367.

(11) Lamberts, S. W. J.; Krenning, E. P.; Reubi, J. C. *Endocrine Rev.* **1991**, *12*, 450−482.

(12) Bauer, W.; Briner, U.; Doepfner, W.; Haller, R.; Huguenin, R.; Marbach, P.; Petcher, T. J.; Pless, J. *Life Sci.* **1982**, *31*, 1133−1140.

(13) Rivier, J.; Brown, M.; Vale, W. *Biochem. Biophys. Res. Commun.* **1975**, *65*, 746−751.

(14) Coy, D. H.; Rossowski, W. J. *Ciba Found. Symp.* **1995**, *190*, 240−252.

(15) Cordelier, P.; Esteve, J. P.; Bousquet, C.; Delesque, N.; O'Carroll, A.; Schally, A. V.; Vaysse, N.; Susini, C.; Buscail, L. *Proc. Natl. Acad. Sci.* **1997**, *94*, 9343−9348.

(16) Papageorgiou, C.; Borer, X. A. *Bioorg. Med. Chem. Lett.* **1996**, *6*, 267−272.

(17) (a) Hirschmann, R.; Nicolaou, K. C.; Pietranico, S.; Salvino, J.; Leahy, E. M.; Sprengeler, P. A.; Furst, G.; Smith, A. B., III, Strader, C. D.; Cascieri, M. A.; Candelore, M. R.; Donaldson, C.; Valle, W.; Maechler, L. *J. Am. Chem. Soc.* **1992**, *114*, 9217−9218. (b) Hirschmann, R.; Nicolaou, K. C.; Pietranico, S.; Leahy, E. M.; Salvino, J.; Arison, B.; Cichy, M. A.; Spoors, P. G.; Shakespeare, W. C.; Sprengeler, P. A.; Hamley, P.; Smith, A. B., III; Reisine, T.; Raynor, K.; Maechler, L.; Donaldson, C.; Vale, W.; Freidinger, R. M.; Cascieri, M. R.; Strader, C. D. *J. Am. Chem. Soc.* **1993**, *115*, 12550−12568.

(18) (a) Yang, L.; Guo, L.; Pasternak, A.; Mosley, R.; Rohrer, S.; Birzin, E.; Foor, F.; Cheng, K.; Schaeffer, J.; Patchett, A. A. *J. Med. Chem.* **1998**, *41*, 2175−2179. (b) Yang, L.; Berk, S. C.; Rohrer, S. P.; Mosley, R. T.; Guo, L.; Underwood, D. J.; Arison, B. H.; Birzin, E. T.; Hayes, E. C.; Mitra, S. W.; Parmar, R. M.; Cheng, K.; Wu, T.; Butler, B. S.; Foor, F.; Paternak, A.; Pan, Y.; Silva, M.; Freidinger, R. M.; Smith, R. G.; Chapman, K.; Schaeffer, J. M.; Patchett, A. A. *Proc. Natl. Acad. Sci. U.S.A.* **1998**, *95*, 10836−10841. (c) Rohrer, S. P.; Birzin, E. T.; Mosley, R. T.; Berk, S. C.; Hutchins, S. M.; Shen, D.; Xiong, Y.; Hayes, E. C.; Parmar, R. M.; Foor, F.; Mitra, S. W.; Degrado, S. J.; Shu, M.; Klopp, J. M.; Cai, S.; Blake, A.; Chan, W.; Pasternak, A.; Yang, L.; Smith, R. G.; Chapman, K. T.; Schaeffer, J. M. *Science* **1998**, *282*, 737−740.

(19) Ankersen, M.; Crider, M.; Liu, S.; Ho, B.; Andersen, H. S.; Stidsen, C. *J. Am. Chem. Soc.* **1998**, *120*, 1368−1373.

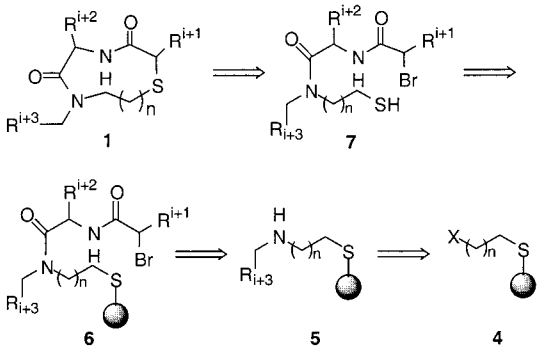

**Figure 4.** Retrosynthesis of turn mimetic **1**.

macrolactamization or intramolecular thioalkylation could be considered. Indeed, due to the limited precedent for preparing strained nine-membered ring lactams through macrocyclization, we had initially explored both strategies toward the synthesis of turn mimetics.[31a] In this initial work, macrolactamization proceeded in poor yields and resulted in considerable quantities of dimer under a variety of reaction conditions. In contrast, thioalkylation proceeded in high yields with minimal dimer or oligomer formation and therefore was selected to prepare heterocycle **1** (Figure 4). We chose to prepare cyclization precursor **7** by solid-phase synthesis to enable an efficient parallel synthesis strategy. The mercaptyl functionality in precursor **7** would serve as the ideal support attachment site, since it would be unmasked for final cyclization upon release from support. Support-bound intermediate **6** would be prepared from secondary amine **5** by sequential coupling of an amino acid to incorporate the $i + 2$ side chain followed by an α-bromo acid to incorporate the $i + 1$ side chain. The $i + 3$ side chain would be introduced by amine displacement upon the activated support-bound backbone **4**. We chose to attach the activated hydroxyalkylthiol backbone element to the solid support through a disulfide linkage rather than a thioether linkage to minimize competitive intramolecular displacement, since disulfides are much poorer nucleophiles than thioethers.

Linker **2** was first prepared by coupling *S*-acetyl 2-mercapto-2-methyl propionic acid[20] to aminomethylated polystyrene resin (Scheme 1). The *gem*-dimethyl substituents adjacent to the sulfur atom are necessary to improve the stability of the eventual disulfide bond. Absence of the *gem*-dimethyl substituents, such as with the analogous 2-mercaptoacetic acid derived linker, results in reduced yields presumably due to the lability of the disulfide bond to amine bases under the forcing conditions used for amine displacement.[21a,b]

Next, methods for attaching the backbone hydroxyalkylthiol to the solid support and activating the hydroxyl for nucleophilic displacement were needed. Methanolysis of thioester **2** followed by disulfide interchange with the methanesulfonoxyalkanethiol backbone component activated as a 2-benzothiazolyl (Bt) mixed disulfide[22] **3** provided mesyl ester **4** (Scheme 1)**.** Completion of the disulfide interchange was monitored by the disappearance of free thiol on the support using Ellman's reagent.[23] Although the backbone component could also be loaded onto the support as the free alcohol followed by conversion to the mesylate with mesyl anhydride and 2,6-lutidine in $CH_2Cl_2$, lower yields of the final mimetics were observed.

**Scheme 1**[a]

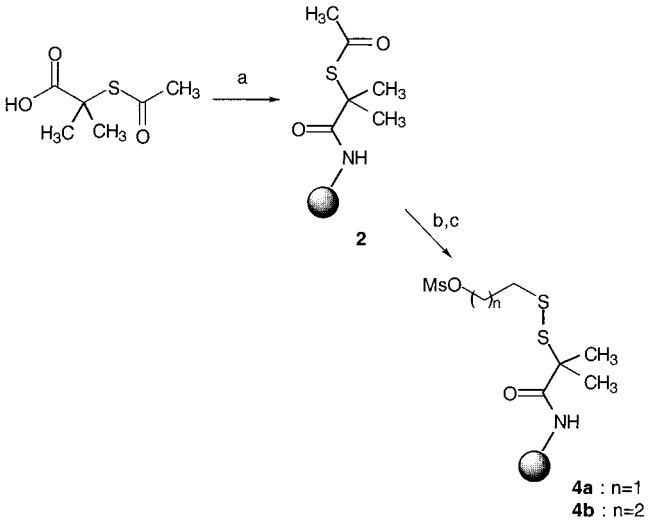

[a] (a) PyBOP, HOBt, *i*-$Pr_2$EtN, aminomethylpolystyrene. (b) NaOMe, 3:1 THF/MeOH. (c) 2-benzothiazolyl 2-methanesulfonoxyalkyl disulfide (**3a or b**).

**Scheme 2**[a]

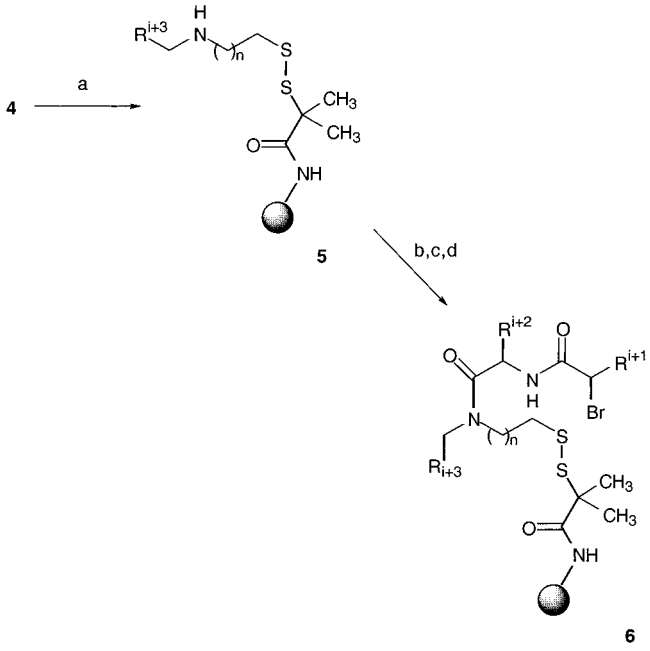

[a] (a) $H_2NCH_2R^{i+3}$, NMP, 55 °C. (b) Fmoc-Amino Acid, HATU, *i*-$Pr_2$EtN, DMF. (c) piperidine (20%), DMF. (d) α-bromo acid, DICI, HOAt, DMF.

The support-bound mesylate **4** was then treated with a concentrated solution of the appropriate primary amine to introduce the $i + 3$ side chain to give **5**. The $i + 2$ side-chain was then incorporated by coupling an Fmoc-protected amino acid. Hydroxyazabenzotriazole based coupling agents were necessary in order to achieve complete coupling with the relatively hindered support-bound secondary amine **5**. Standard Fmoc deprotection and subsequent coupling with an α-bromo acid to incorporate the $i + 1$ side chain provided the support-bound cyclization precursor **6** (Scheme 2).

A key challenge in the synthesis of mimetic **1** was to develop appropriate support release and cyclization steps for the parallel synthesis of the pure mimetics. We initially used the volatile reagents triethyl phosphine and *N*-methyl morpholine (NMM) to reduce the support-bound disulfide and drive the cyclization,

(20) Mery, J.; Brugidou, J.; Derancourt, J. *J. Pept. Res.* **1992**, *5*, 223−240.

(21) (a) Mery, J.; Granier, C.; Juin, M.; Brugidou, J. *Int. J. Pept. Protein Res*. **1993**, *42*, 44−52. (b) Greene, T. W.; Wuts, P. G. M. *Protective Groups in Organic Synthesis*; John Wiley & Sons: New York, 1991; pp 438−440.

(22) Brzezinska, E.; Ternay, A. L. *J. Org. Chem.* **1994**, *59*, 8239−8244.

(23) Ellman, G. L. *Arch. Biochem. Biophys*. **1959**, *82*, 70−77.

**Scheme 3**[a]

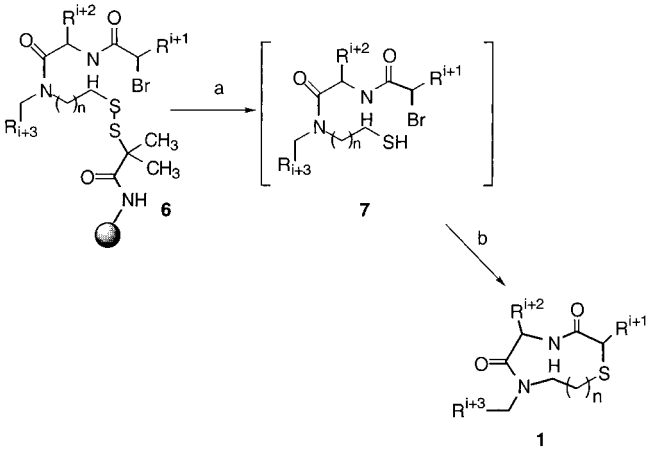

[a] (a) TCEP. (b) 1% divinylbenzene-polystyrene-*N*,*N*,*N*,*N*-tetramethylguanidine resin.

respectively, since they could be removed by concentration in vacuo. However, while the volatile reagents could be removed, the triethyl phosphine oxide and *N*-methyl morpholine hydrobromide byproducts contaminated the final turn mimetics after concentration. These contaminants complicated analytical characterization of the compounds and had the potential to interfere with biological evaluation. We therefore developed a solid-phase extraction approach for the rapid removal of HBr and phosphine impurities.

A support-bound amine could easily be used in place of a tertiary amine to scavenge HBr; however, a suitable support-bound reagent could not be identified that would scavenge the triethylphosphine oxide. We therefore employed the modified phosphine reagent tris-(2-carboxyethyl)phosphine (TCEP) to reduce the disulfide. Both excess TCEP and the oxide should be scavenged by the same support-bound amine that was used to scavenge HBr.[24] Support-bound *N*,*N*,*N*,*N*-tetramethylguanidine (TMG) proved to be the optimal scavenging reagent because it served both as an effective solid-phase extraction resin and as a general base to promote thioether formation to yield cyclic product **1**. Cyclization with the support-bound guanidine proceeded to completion within 24 h at room temperature. Furthermore, the formation of cyclic dimer or oligomers was not observed when the cyclization reaction was performed at 1 mM substrate concentrations. Filtration to remove the resin followed by concentration in vacuo yielded the crude product **1** uncontaminated with reagent byproducts (Scheme 3). The preliminary publication of this work marked the first use of solid-phase synthesis and solid-phase extraction in the same synthesis sequence and represented one of the first applications of solid-phase extraction methods for the synthesis of compound libraries.[6]

Seven mimetics **1(a**−**g)** were prepared to demonstrate the generality of the synthesis sequence. High levels of purity (>90%) as determined by HPLC and $^1$H NMR were observed for each of the crude mimetics obtained directly from the resin. In addition, the average overall yield for the chromatographed and analytically pure material was 59% based upon the expected loading of **2** (Table 1). The only identifiable side-products (≤5%) were the minor diastereomers corresponding to inversion at the α-carbon at the $i + 1$ position. This most likely results from the initial optical purity of the α-bromo acids that supply the $i + 1$ side chain (generally ∼95% ee as determined by chiral GC or HPLC analysis), although a small amount of racemization

**Table 1.** Synthesis of β-turn Mimetics[a]

| | $R^{i+1}$ | $R^{i+2}$ | $R^{i+3}$ | n | purity (crude) | yield (purified) |
|---|---|---|---|---|---|---|
| 1a |  |  | 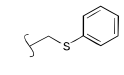 | 1 | 92 | 60 |
| 1b | (*S*)  |  | 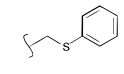 | 1 | 94 | 64 |
| 1c |  | 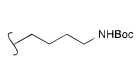 | 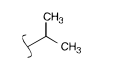 | 1 | 86 | 56 |
| 1d |  | 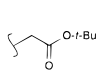 | 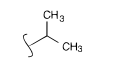 | 1 | 93 | 61 |
| 1e |  |  | 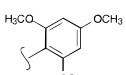 | 2 | 94 | 51 |
| 1f | (*S*) 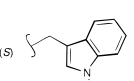 | 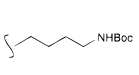 | 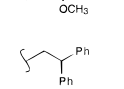 | 1 | 84 | 59 |
| 1g | (*S*) 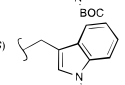 (*R*) | 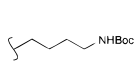 | 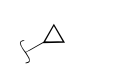 | 1 | 93 | 59 |

[a] The stereochemical configuration of the α-carbon at the $i + 1$ site is *R* and at the $i + 2$ site is *S* unless otherwise specified. The purity of the crude product directly off of the support was determined by reverse phase HPLC, 60−100% $CH_3OH$ in 0.1% aqueous TFA as monitored at 220, 254, or 280 nM.

during the synthesis sequence cannot be ruled out. The successful introduction of the functionalized lysine, aspartic acid, and tryptophan side chains, nine- and ten-membered ring sizes, and both stereochemistries at the $i + 1$ and $i + 2$ sites clearly demonstrates the broad generality of the synthesis sequence.

**Design and Synthesis of Mimetic Library Targeting Somatostatin.** A focused library of somatostatin mimetics (Figure 5) was designed based upon prior, extensive studies of peptide analogues of somatostatin.[25a−c] Other active cyclic peptides include a retro-enantio analogue[26a,b] of somatostatin wherein both the order and stereochemistry of the central Trp and Lys residues are reversed. These examples indicated that several alternative displays of the tryptophan and lysine side chains could potentially provide active compounds. For this reason all eight possible combinations of the Trp and Lys side chains of both stereochemistries were included at the $i + 1$ and $i + 2$ positions. Twenty-two different amines were introduced at the $i + 3$ position. Eight of the amines were chosen for their their similarity to the $i + 3$ (Phe and Tyr) as well as the i (Thr and Val) residues present in numerous somatostatin analogues. The remaining 14 amines were selected to maximize the diversity of functionality at this site employing a heirarchical, 2D structure key-based clustering algorithm developed by MDL Information Systems.[27]

(24) Burns, J. A.; Butler, J. C.; Moran, J.; Whitesides, G. M. *J. Org. Chem.* **1991**, *56*, 2648−2650.

(25) (a) Brady, S. F., Paleveda, W. J.; Arison, B. H.; Saperstein, R.; Brady, E. J.; Raynor, K.; Reisine, T.; Veber, D. F.; Freidinger, R. M. *Tetrahedron* **1993**, *49*, 3449−3466. (b) Veber, D. F.; Saperstein, R.; Nutt, R. F.; Freidinger, R. M.; Brady, S. F.; Curley, P.; Perlow, D. S.; Paleveda, W. J.; Colton, C. D.; Zacchei, A. G.; Tocco, D. J.; Hoff, D. R.; Vandlen, R. L.; Gerich, J. E.; Hall, L.; Mandarino, L.; Cordes, E. H.; Anderson, P. S.; Hirschmann, R. *Life Sci.* **1984**, *34*, 1371−1378. (c) Hocart, S. J.; Reddy, V.; Murphy, W. A.; Coy, D. H. *J. Med. Chem.* **1995,** *38*, 1974−1989.

(26) (a) Pallai, P.; Struthers, S.; Goodman, M.; Rivier, J.; Vale, W. *Biopolymers* **1983**, *22*, 2523−2538. (b) Murphy, W. A.; Heiman, M. L.; Lance, V. A.; Mezo, I.; Coy, D. H. *Biochem. Biophys. Res. Commun.* **1985**, *132*, 922−928.

(27) Muskal, S. Unpublished Results. MDL Information Systems, Inc., San Leandro, CA.

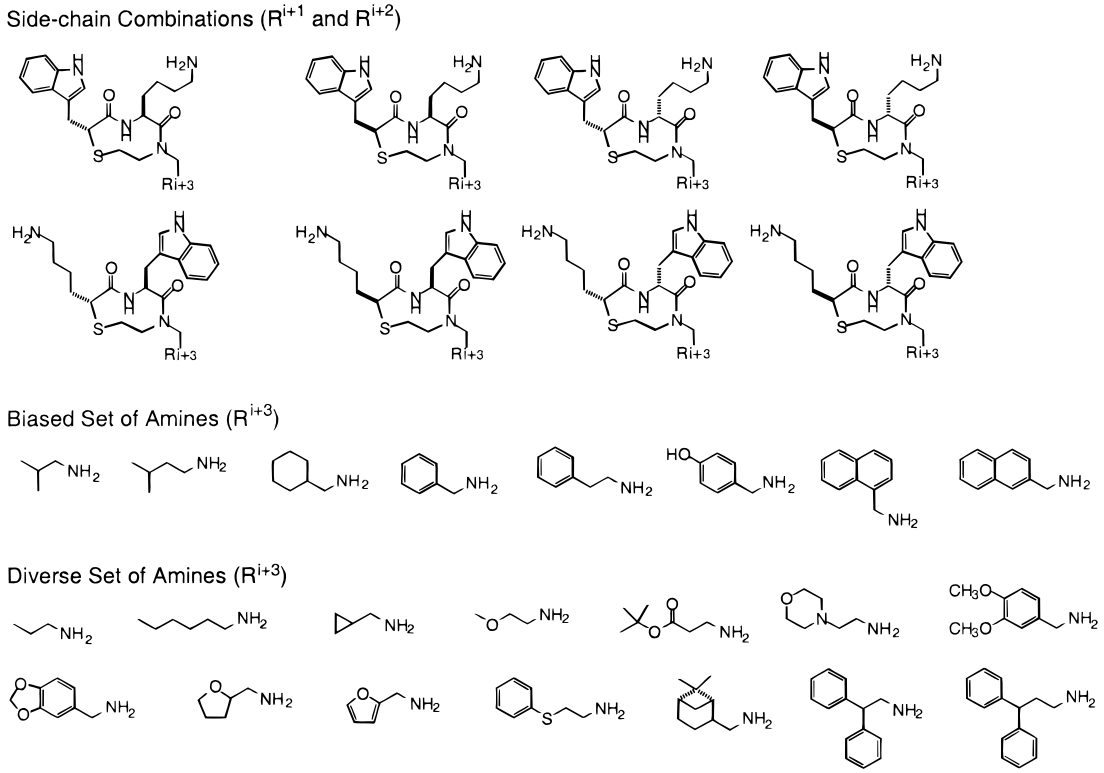


**Figure 5.** Focused library of somatostatin mimetics.

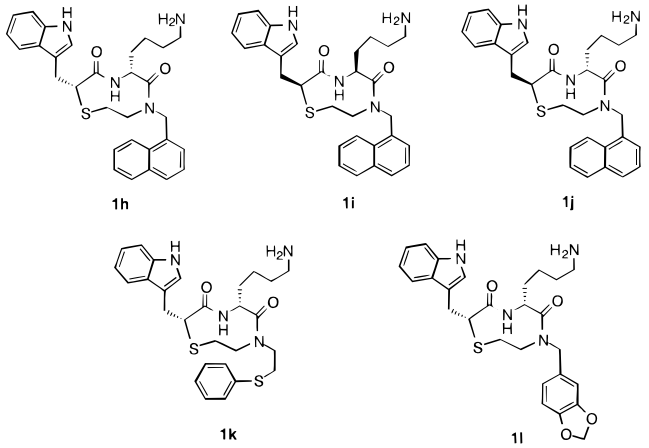


**Figure 6.** Scaled-up somatostatin ligands.

Each compound was then screened against all five cloned human somatostatin receptor subtypes. The ability of the compounds to inhibit the binding of [$^{125}$I]-Tyr11-SRIF to human recombinant $SST_1$, $SST_3$, $SST_4$, and $SST_5$ and the binding of [$^{125}$I]-BIM-23027 to the human recombinant $SST_2$ all expressed in CHO-K1 cells was measured. The compounds that showed the greatest inhibition of specific binding were then tested at lower concentrations in order to more accurately define their potency. The most active compounds targeting $hSST_2$, $hSST_3$, and $hSST_5$, **1k**, **1l**, and **1h**, respectively, were prepared on a larger scale for exact $IC_{50}$ determinations on fully characterized and purified material (Figure 6). The two stereoisomers, **1i** and **1j**, of the most potent ligand to $hSST_5$, **1h**, showed modest activity in the library screen. These compounds were also prepared on a large scale for exact $IC_{50}$ determinations in order to further assess the impact of stereochemistry on binding.

**Intepretation of assay results.** The binding data clearly established the preference for Trp at the $i + 1$ position and Lys at the $i + 2$ position, which corresponds to the sequence found in somatostatin. The screening data also clearly indicated that the preferred stereochemistry at the $i + 1$ and $i + 2$ positions is of D configuration (Table 1). While the selection of D-Trp is not surprising given the large number of potent cyclic peptide analogues of somatostatin that incorporate D-Trp at the $i + 1$ position,[25a−c] Lys of L-configuration is clearly preferred at the $i + 2$ position in peptides.[28] Additionally, large aromatic groups are preferred at the $i + 3$ position of heterocycle **1**. This result is consistent with the clear requirement for hydrophobic contacts in peptide analogues of somatostatin,[29] although it would not have been predicted based upon the preference for Val or Thr at the $i + 3$ position of the peptide analogues. The unexpected binding preference for D-Lys at the $i + 2$ position, which has been observed once before in a cyclic peptide somatostatin analogue,[30] and the large aromatic groups at the $i + 3$ position highlight the importance of evaluating multiple mimetics with varied side-chain displays even when the structures are modeled on an extensively studied peptide such as somatostatin.

The effect of stereochemistry on bioactivity is highlighted in Table 2. Mimetic **1h** exhibits remarkable potency toward $SST_5$, while the activity of $i + 2$ epimer **1j** toward the same subtype decreases by nearly 15-fold. Furthermore, the activity of the *S,S* enantiomer **1i** also shows a considerable decrease toward $hSST_5$. It is further interesting to note that heterocycle **1h** also exhibits the highest level of selectivity, with its affinity for $hSST_5$ being greater than 10-fold over that of subtypes 2−4, and nearly 10-fold over $hSST_1$. Finally, heterocycles **1k** and **1l** were found to be the most potent toward subtypes 2 and 3,

(28) Nutt, R. F.; Veber, D. F.; Curley, P. E.; Saperstein, R.; Hirschmann, R. F. *Int. J. Pept. Protein Res.* **1983**, *21*, 66−73.

(29) Nutt, R. F.; Saperstein, R.; Veber, D. F. *Peptides - Structure & Function. Proceedings of the Eighth American Peptide Symposium*; Hruby, V. J., Rich, D. H., Eds.; Pierce Chemical Co.: Rockford, Il, 1983; pp 345−348.

(30) Freidinger, R. M.; Veber, D. F. In *Conformationally Directed Drug Design*: Vida, J. A., Gordon, M., Eds.; ACS Symposium Series 251; American Chemical Society: Washington, DC, 1984; pp 169−187.

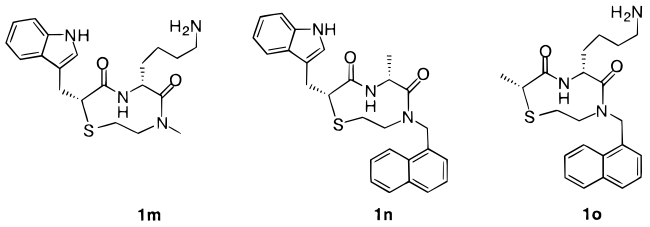


**Figure 7.** Alanine scan derivatives of ligand **1h**.

**Table 2.** $IC_{50}$ Values (nM) for the Most Potent Somatostatin Mimetics (values reflect assay results of purified material)

| ligand | hSST1 | hSST2 | hSST3 | hSST4 | hSST5 |
|---|---|---|---|---|---|
| **1h** | 501 | 1585 | 3090 | 1047 | 87 |
| **1i** | 2240 | 3630 | 813 | 363 | 832 |
| **1j** | 4467 | 4571 | 1202 | 3162 | 1202 |
| **1k** | 1096 | 158 | 1175 | 479 | 589 |
| **1l** | 851 | 252 | 135 | 245 | 120 |

respectively, with the latter compound also showing affinity for three of the remaining four subtypes ($hSST_2$, $hSST_4$, and $hSST_5$).

To further establish that each side chain plays an important role in recognition, three derivatives of the most potent ligand **1h** ($IC_{50} = 87$ nM to $hSST_5$) were prepared with each derivative having one of the three side chains replaced with a methyl substituent (Figure 7). None of the derivatives showed significant binding to $hSST_5$ ($IC_{50} > 10$ $\mu$M) unambiguously establishing the importance of each side chain for binding.

**Synthesis and Evaluation of an $i + 3$ Diversity Library.** A second series of mimetics was then prepared based upon the structures of the most potent compounds targeting $hSST_2$ and $hSST_5$. The $i + 1$ and $i + 2$ side chains were fixed as the Trp/Lys side chains, respectively, both with D-stereochemistry (Figure 8). To introduce the $i + 3$ side chain, 16 amines containing aromatic functionality were selected based upon structual similarity to those amines that resulted in heterocycles of greatest activity from the first library. Biological evaluation of this small collection of heterocycles established that a majority of the compounds had submicromolar $IC_{50}$ values. However, none of the incorporated $i + 3$ side chains resulted in improved activity toward either $hSST_2$ or $hSST_5$.

We anticipate that significant improvement in affinity and specificity may yet be achieved. Evaluation of much larger collections of amines at the $i + 3$ position could result in improved binding to $hSST_2$ or $hSST_5$, while modifications that enhance the rigidity of the heterocycle and of the side chain display may also provide enhanced affinity and particularly specificity. Multiple low-energy conformers of heterocycle **1h** are likely populated based upon molecular modeling and NMR analysis of **1** and of earlier mimetic structures,[6,31a−c] and introduction of constrained backbone elements or cyclic amino acid derivatives at the $i + 2$ position will signicantly reduce the conformational flexibility of heterocyle **1h**. Finally, the $i + 1$ and $i + 2$ side chains can also be biased by introduction of $\beta$-methyl-substituted side chains. Related approaches have successfully been employed to greatly enhance the affinity and specificity of peptide ligands.[32a,b]

(31) (a) Virgilio, A. A.; Ellman, J. A. *J. Am. Chem. Soc.* **1994,** *116*, 11580−11581. (b) Virgilio, A. A.; Bray, A. A.; Zhang, W.; Trinh, L.; Ellman, J. A. *Tetrahedron* **1997**, *53*, 6635−6644. (c) Virgilio, A. A. 1997. The Design, Synthesis, and Evaluation of Libraries of $\beta$-Turn Mimetics. Ph. D. Dissertation, University of California, Berkeley, CA.

(32) (a) Liao, S.; Shenderovich, M. D.; Zhang, Z.; Maletinska, L.; Slaninova, J.; Hruby, V. J. *J. Am. Chem. Soc.* **1998**, *120*, 7393−7394. (b) Haskell-Leuvano, C.; Toth, K.; Boteju, L.; Job, C.; Castrucci, A. M.; Hadley, M. E.; Hruby, V. J. *J. Med. Chem.* **1997**, *40*, 2740−2749.

## Conclusion

The identification of peptidomimetics is an important goal to many academic and industrial researchers. The design and synthesis of peptidomimetic scaffolds based on the $\beta$-turn structure has received the most attention due to the importance of this secondary structural motif in peptide and protein recognition. However, despite considerable effort, very few bioactive small molecule $\beta$-turn mimetics have been developed due to the difficulty of determining the identity and orientation of key side chains.

Herein we report the first successful application of a *designed* combinatorial library of $\beta$-turn mimetics. The synthesis and screening of a 172-member library of medium-ring heterocycles incorporating the side-chain display observed in the critical $\beta$-turn present in cyclic peptide analogues of somatostatin resulted in the identification of an 87 nM ligand **(1h)** to $hSST_5$. Central to the success of these efforts was the cability of preparing heterocycles displaying different side chains corresponding to the $i + 1$, $i + 2$ and $i + 3$ positions of the $\beta$-turn, in addition to different side chain stereochemistries. Unanticipated side chains and stereochemistries were identified in this study demonstrating the critical importance of evaluating collections of mimetics. Further optimization of specificity and affinity will be attempted through the parallel synthesis and evaluation of constrained mimetics. Finally, using the methods described herein, a large library of turn mimetics that incorporate all of the proteinogenic amino acid side chains at the $i + 1$, $i + 2$, and $i + 3$ positions has been prepared.[31c] Screening this library should prove to be ideal for the identification of peptidomimetic ligands to receptors where relatively little information is available regarding receptor−peptide ligand interactions.[1]

## Materials and Methods

**Reagents and General Methods.** Unless otherwise noted, all reagents were obtained from commercial suppliers and used without further purification. When used as a reaction solvent, $CH_2Cl_2$ was distilled from $CaH_2$, and THF and dioxane were distilled under $N_2$ from sodium benzophenone ketyl, all immediately prior to use. Deoxygenation of solvents and reaction mixtures was achieved by bubbling $N_2$ or Ar through them for 15−20 min. *N*-Fmoc-protected amino acids, Merrifield chloromethyl resin, and aminomethyl polystyrene resin were purchased from Calbiochem-Novabiochem Corp. (San Diego, CA) or Bachem Bioscience Inc. (King of Prussia, PA). α-Bromo acids were prepared in one step in optically enriched form acccording to the recently published procedure.[8]

Chromatography was carried out using Merck 60 230−240 mesh silica gel according to the procedure described by Still.[33] Components were visualized either by ultraviolet light or anisaldehyde staining.[34] Melting points were determined in open Pyrex capillaries and are uncorrected. NMR spectra were recorded on Bruker AMX 300, AMX 400, AM 400, or AM 500 machines. Samples for NMR analysis that contained rotamers were heated to cause coalescence of the different rotameric peaks. NMR chemical shifts are expressed in ppm downfield, relative to internal solvent peaks. Coupling constants, *J*, are listed in hertz. When $^{31}P$ NMR spectra were obtained, the chemical shifts were calibrated on tetramethyl phosphate as an internal standard at 3.08 ppm. Reverse phase HPLC was performed on a DynamaxŒ HPLC system from Rainin using a Microsorb $C_{18}$ column from Rainin and a flow rate of 1 mL/min with methanol/water 0.1% TFA as the mobile phase. MALDI-TOF mass spectrometry was performed on a Voyager Bio-Spectrometry workstation. Infrared spectra were recorded on a Perkin-Elmer 1600 FT-IR spectrophotometer, either taken as thin films on NaCl plates or as KBr pellets. Elemental analyses were performed by

(33) Still, W. C.; Kahn, M.; Mitra, A. *J. Org. Chem.* **1978**, *43*, 2923.

(34) Gordon, A. J.; Ford, R. A. *The Chemist's Companion*; John Wiley & Sons: New York, 1972; pp 378−380.

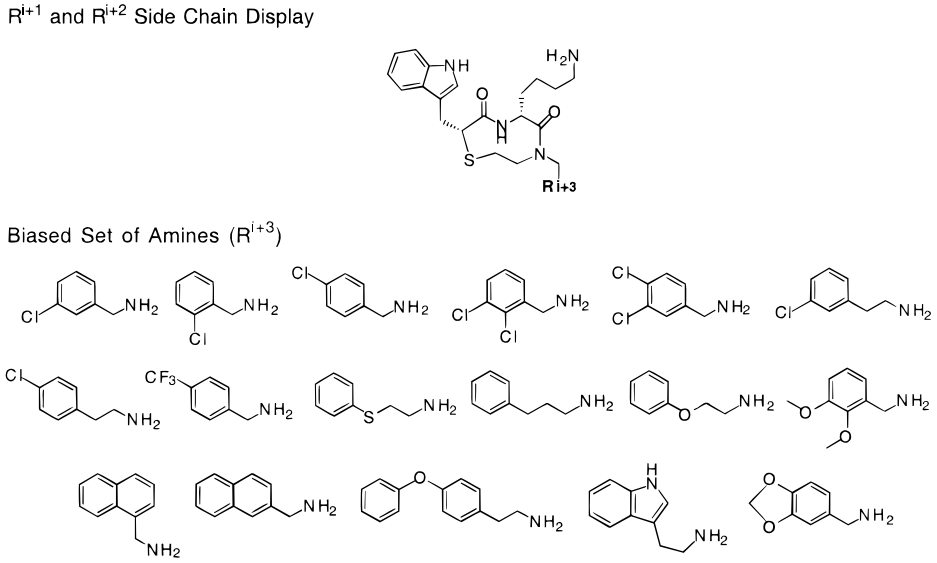


**Figure 8.** $R^{i+3}$ diversification library.

M-H-W Laboratories (Phoenix, AZ) or by the Microanalytical Laboratory at the University of California at Berkeley.

**Preparation of Disulfide Methanesulfonate Linkers (3a,b).** Modifications were made to the procedure reported by Brzezinska and Ternay for the preparation of 2-benzothiazolyl disulfides[22] since the purity and yield could not be reproduced in our hands. 2,2′-Dithiobis(benzothiazole) (73.2 g, 220 mmol) was placed in a 5-L three-necked round-bottom flask and dissolved in 3 L of chloroform with heating and mechanical stirring. After all of the 2,2′-dithiobis(benzothiazole) had dissolved, the solution was allowed to cool to room temperature. Over a period of 2 h β-mercaptoethanol (14 mL, 200 mmol) in 500 mL of chloroform was then added with an addition funnel. The reaction solution was stirred for an additional 2 h and then extracted with 5% NaOH (aqueous) (2 × 300 mL) and brine (2 × 300 mL). The chloroform layer was dried ($MgSO_4$), and the solvent was removed by concentration in vacuo. To remove unreacted 2,2′-dithiobis(benzothiazole), the crude product was suspended in 700 mL of methanol and refluxed with stirring for 30 min. The mixture was slowly cooled to 4 °C and maintained at 4 °C overnight. The crystallized 2,2′-dithiobis-(benzothiazole) was removed by suction filtration and rinsed with cold methanol. The methanol solution was concentrated in vacuo to yield 41.2 g (170 mmol, 85%) of a bright yellow solid which was used without further purification. Mp 65 °C [lit. mp 69−71 °C].[22] $^1$H NMR (300 MHz, $CDCl_3$) $\delta$ 3.07 (t, 2, $J$ = 5.4), 3.91 (dt, 2, $J$ = 6.8, 5.4), 4.46 (t, 1, 6.8), 7.34 (td, 1, $J$ = 8.0, 1.2), 7.45 (td, 1, $J$ = 8.0, 1.2), 7.77 (dd, 1, $J$ = 8.0, 1.2), 7.90 (dd, 1, $J$ = 8.0, 1.2).

2-Benzothiazolyl 2-hydroxyethyl disulfide (32 g, 132 mmol) in 500 mL of methylene chloride was cooled to 0 °C, and 31 mL (263 mmol) of 2,6-lutidine was added with mechanical stirring. Methanesulfonyl anhydride (35.4 g, 197 mmol) was added in portions over 15 min. The reaction mixture was then allowed to warm to room temperature while stirring. When no starting material was left (0.3 h as determined by TLC), the reaction mixture was washed with 1 N HCl (aqueous) (2 × 500 mL), 1 N NaOH (aqueous) (2 × 500 mL), and brine (2 × 500 mL) and dried ($MgSO_4$) and concentrated in vacuo. Purification by column chromatography, eluting first with 7:1:2 hexanes/dichloroethane/ethyl acetate, and then gradually increasing the dichloroethane and ethyl acetate content, gave 37.6 g (117 mmol, 89%) of product **3a** as white crystals: $^1$H NMR (300 MHz, $CDCl_3$) $\delta$ 3.04 (s, 3H), 3.29 (t, 2, $J$ = 6.4), 4.55 (t, 2, $J$ = 6.4), 7.36 (td, 1, $J$ = 8.0, 1.2), 7.46 (td, 1, $J$ = 8.0, 1.2), 7.82 (dd, 1, $J$ = 8.0, 1.2), 7.90 (dd, 1, $J$ = 8.0, 1.2). $^{13}$C NMR (300 MHz, $CDCl_3$) $\delta$ 37.7, 38.0, 66.6, 121.2, 122.4, 125.0, 126.5, 135.9, 154.7, 170.2. Anal. Calcd for $C_{10}H_{11}NO_3S_4$ C, 37.36; H, 3.45; N, 4.36. Found C, 37.50; H, 3.28; N, 4.12.

**(3b):** 81%. $^1$H NMR (400 MHz, $CDCl_3$) $\delta$ 2.19 (tt, 2, $J$ = 7.0, 5.9), 2.98 (s, 3H), 3.04 (t, 2, $J$ = 7.0), 4.33 (t, 2, $J$ = 5.9), 7.31 (td, 1, $J$ = 8.0, 1.2), 7.41 (td, 1, $J$ = 8.0, 1.2), 7.78 (dd, 1, $J$ = 8.0, 1.2), 7.84 (dd, 1, $J$ = 8.0, 1.2). $^{13}$C NMR (400 MHz, $CDCl_3$) $\delta$ 28.3, 34.9, 37.2, 67.4, 121.1, 122.0, 124.6, 126.2, 135.6, 154.7, 171.3. Anal. Calcd for $C_{11}H_{13}NO_3S_4$ C, 39.38; H, 3.91; N, 4.18. Found C, 39.36; H, 4.04; N, 3.96.

**Tris(2-carboxyethyl)phosphine.** The preparation of tris(2-carboxyethyl)phosphine[24] was altered so as to afford the neutral compound rather than the hydrochloride salt. Tris(2-cyanoethyl)phosphine (92% purity, 8% phosphine oxide) was purchased from Strem Chemicals. Tris(2-cyanoethyl)phosphine (25 g, 119 mmol) was refluxed under a $N_2$ atmosphere in 85 mL of concentrated HCl (aqueous) for 3 h. The solution was cooled to room temperature, and 100 mL of deoxygenated water followed by 16.1 g (643 mmol) of NaOH in 100 mL of deoxygenated water were added while a nitrogen atmosphere was maintained. The solution was extracted with oxygen-free THF (3 × 500 mL). The combined THF extracts were concentrated in vacuo to obtain crystals which were dried under high vacuum to give 21 g (76 mmol, 64%) of 90% pure (10% phosphine oxide) tris(2-carboxyethyl)-phosphine. $^1$H NMR (400 MHz, $d_6$-DMSO) $\delta$ 1.60 (t, 6, $J$ = 7.9), 2.28 (dt, 6, $J$ = 9.4, 7.9), 9.44 (br s, 3). $^{13}$C NMR (400 MHz, $d_6$-DMSO) $\delta$ 27.8 (d, $J$ = 13.0), 33.7 (d, $J$ = 15.5), 123.2 (d, $J$ = 10.8). $^{31}$P NMR (400 MHz, $d_6$-DMSO): $\delta$ −26.3.

**Preparation of *N,N,N,N*-Tetramethylguanidine Resin.** To 25 g of 200−400 mesh Merrifield chloromethyl resin (1.0 mmol/g, 25 mmol) was added a 1.0 M solution of tetramethylguanidine (25 mL, 250 mmol) in $CH_2Cl_2$ (150 mL). Catalytic tetrabutylammonium iodide was added, and the reaction slurry was heated to reflux for 14 h. The reaction mixture was transferred to a fritted glass funnel, and the resin was rinsed exhaustively with $CH_2Cl_2$ (2 × 200 mL), 3:1:1 THF/MeOH/1 N NaOH (aqueous) (5 × 200 mL), THF (2 × 200 mL), and MeOH (2 × 200 mL). The resin was then dried in vacuo. No detectable amount of chloride remained on the resin as indicated by the Beilstein test and Vollhard titration.[35] Combustion analysis was performed to determine nitrogen content. Anal. Calcd N, 3.9 (0.93 mequiv/g). Found N, 2.2 (0.52 mequiv/g).

**General Procedure for the Solid-Phase Synthesis of β-Turn Mimetics 1.** Aminomethyl-derivatized polystyrene resin is solvated in DMF (10 mL/g of resin), and *S*-acetyl 2-mercapto-2-methyl propionic acid (0.2 M), PyBOP (0.2 M), HOBt (0.2 M), and *i*-$Pr_2$EtN (0.4 M) are added. After 8 h, the solution is drained, and the resin is rinsed with DMF (3×), $CH_2Cl_2$ (4×), and MeOH (2×), then dried in vacuo. Resin **2** is then solvated in a 3:1 THF/MeOH mixture (10 mL/g of resin) and purged with Ar (20 min). NaOMe is added to reach a final concentration of 0.2 M, and the reaction vessel is stoppered and shaken for 1 h. Excess AcOH is added to quench the reaction, and the resin is isolated by filtration. The resin is rinsed with 3:1 THF/MeOH (2×) and $CH_2Cl_2$ (3×). A 0.1 M solution of the benzothiazolyl-activated disulfide mesylate **3a** in $CH_2Cl_2$ is added to the resin, and the reaction

(35) Vogel, A. I. *Vogel's Textbook of Quantitative Inorganic Analysis*, 4th ed.; Longmans: London, 1978; pp 342.

vessel is stoppered under an Ar atmosphere. After 12 h, the resin is isolated by filtration and rinsed with $CH_2Cl_2$ (5×) and MeOH (2×) to afford **4.** The mesylate **4** is treated with a 1.0 M solution of the desired amine in NMP for 16 h at 50 °C. The resin is isolated by filtration and rinsed with DMF (3×), $CH_2Cl_2$ (5×), and MeOH (2×) to give **5**. Resin **5** is solvated in DMF (10 mL/g of resin) and the desired Fmoc-protected amino acid (0.2 M), HATU (0.2 M), and *i*-$Pr_2EtN$ (0.4 M) are added. After 8 h, the resin is collected by filtration and rinsed with DMF (3×), $CH_2Cl_2$ (5×), and MeOH (2×). A solution of piperidine (20% v/v) in DMF is used to deprotect the resin (20 min), and it is rinsed as before. The deprotected resin is solvated in DMF (10 mL/g of resin) and the desired α-bromo acid, HOAt (0.1 M), and DICI (0.1 M) are added. After 4 h, the resin is isolated by filtration and rinsed as above to provide **6**. The disulfide linkage of **6** to the solid support is reduced by treatment with a 3.0 mM solution of TCEP in a 9:1 dioxane/$H_2O$ solution (1 mL/mmol of resin bound **6**), which has been purged with Ar (20 min). After 8 h, the solution of acyclic turn mimetic is transferred via a filtration cannula and under Ar pressure to a flask containing ~30 equiv of support-bound tetramethyl guanidine. After the disappearance of all of the acyclic material (<24 h as determined by HPLC), the solution is filtered to remove the resin and the filtrate is concentrated in vacuo to yield crude **1**. The crude mimetics (**1**) were purified for analysis by column chromatography on silica gel using EtOAc/hexane mixtures as the eluant.

**Determination of the Expected Loading of Linker (2).** Aminomethyl polystyrene resin (100 mg) was acylated with Fmoc-Aib-OH (65 mg, 0.20 mmol) using PyBOP (104 mg, 0.20 mmol), HOBt (27 mg, 0.20 mmol), *i*-$Pr_2EtN$ (70 mL, 0.40 mmol) in 1 mL of DMF. The conditions were identical to those used to load the linker precursor, *S*-acetyl 2-mercapto-2-methyl propionic acid. Fmoc-Aib-OH should couple to the aminomethyl resin similar to *S*-acetyl 2-mercapto-2-methyl propionic acid since both have two geminal methyl substituents on the α-carbon. The loading level of the resin (negative to bromophenol blue) was then determined by spectrophotometric quantitation of the Fmoc chromophore to be 0.50 ± 0.02 mequiv/g.[36]

**(1a):** $^1$H NMR ($d_6$-DMSO, 300 MHz, 75 °C) $\delta$ 0.91 (m, 6), 1.17 (d, 3, $J$ = 6.6), 1.37 (m, 1), 1.59 (m, 1), 1.68 (m, 1), 2.85−3.37 (m, 7), 3.52 (q, 1, 6.6), 3.60 (m, 1), 4.52 (m, 1), 7.19 (t, 1, $J$ = 7.4), 7.31 (t, 2, $J$ = 7.4), 7.38 (d, 2, $J$ = 7.4), 8.48 (d, 1, $J$ = 9.5). LRMS (MALDI-TOF) mass calcd for $C_{19}H_{29}N_2O_2S_2$ ($MH^+$) 381.2. Found 381.3. Anal. Calcd for $C_{19}H_{28}N_2O_2S_2$ C, 59.96; H, 7.42; N, 7.36. Found C, 59.99; H, 7.56; N, 7.21.

**(1b):** $^1$H NMR ($d_6$-DMSO, 300 MHz, 75 °C) $\delta$ 0.90 (d, 6, $J$ = 6.2), 1.18−1.70 (m, 6), 2.70−3.57 (m, 8), 3.87 (m, 1), 4.61 (m, 1), 7.18 (t, 1, $J$ = 7.5), 7.31 (t, 2, $J$ = 7.5), 7.39 (d, 2, $J$ = 7.5), 8.00 (m, 1). LRMS (MALDI-TOF) mass calcd for $C_{19}H_{29}N_2O_2S_2$ ($MH^+$) 381.2. Found 381.3. Anal. Calcd for $C_{19}H_{28}N_2O_2S_2$ C, 59.96; H, 7.42; N, 7.36. Found C, 59.71; H, 7.27; N, 7.17.

**(1c):** $^1$H NMR ($d_6$-DMSO, 300 MHz, 75 °C) $\delta$ 0.77 (d, 3, $J$ = 6.7), 0.84 (d, 3, $J$ = 6.7), 1.17 (d, 3, $J$ = 6.6), 1.25−1.42 (m, 5), 1.37 (s, 9), 1.78−1.93 (m, 2), 2.71−2.78 (m, 1), 2.87−3.09 (m, 4), 3.18−3.41 (m, 3), 3.60 (q, 1, $J$ = 6.6), 4.52 (m, 1), 6.36 (m, 1), 8.58 (d, 1, $J$ = 9.4). LRMS (MALDI-TOF) mass calcd for $C_{20}H_{37}N_3O_4SNa$ ($MNa^+$) 438.2. Found 438.6. Anal. Calcd for $C_{20}H_{37}N_3O_4S$ C, 57.80; H, 8.97; N, 10.11. Found C, 57.72; H, 8.82; N, 9.91.

**(1d):** $^1$H NMR ($d_6$-DMSO, 300 MHz, 75 °C) $\delta$ 0.77 (d, 3, $J$ = 6.7), 0.86 (d, 3, $J$ = 6.7), 1.38 (s, 9), 1.90 (m, 1), 2.32 (m, 1), 2.55−3.10 (m, 5), 3.24.3.40 (m, 4), 4.97 (m, 1), 8.60 (m, 1). Anal. Calcd for $C_{16}H_{28}N_2O_4S$ C, 55.79; H, 8.19; N, 8.13. Found C, 56.06; H, 8.38; N, 7.92.

**(1e):** $^1$H NMR ($d_6$-DMSO, 400 MHz, 75 °C) $\delta$ 0.97 (d, 3, $J$ = 6.6), 1.03 (d, 3, $J$ = 6.6), 1.24 (d, 3, $J$ = 6.3), 1.94 (m, 1), 2.16 (m, 1), 2.38−2.50 (m, 3), 3.16 (m, 1), 3.33 (m, 1), 3.75 (m, 1), 3.78 (s, 3), 3.79 (s, 6), 4.40 (m, 1), 4.48 (m, 1), 5.27 (m, 1), 6.26 (s, 2), 8.06 (m, 1). LRMS (MALDI-TOF) mass calcd for $C_{21}H_{33}N_2O_5S$ ($MH^+$) 425.2. Found 4252.

**(1f):** $^1$H NMR ($d_6$-DMSO, 300 MHz, 75 °C) $\delta$ 0.1.14 (m, 2), 1.36 (s, 9), 1.63 (s, 9), 1.25−1.65 (m, 3), 1.78 (m, 1), 2.27 (m, 2), 4.10 (m, 1), 4.37 (m, 1), 4.74 (m, 1), 6.36 (m, 1), 7.13−7.34 (m, 12), 7.49 (m, 1), 7.65 (m, 1), 8.01 (d, 1, $J$ = 8.1), 8.13 (m, 1). LRMS (MALDI-TOF) mass calcd for $C_{44}H_{57}N_4O_6S$ ($MH^+$) 769.4. Found 769.4. Anal. Calcd for $C_{44}H_{56}N_4O_6S$ C, 68.72; H, 7.34; N, 7.29. Found C, 68.38; H, 7.21; N, 7.21.

**(1 g):** $^1$H NMR ($d_6$-DMSO, 300 MHz, 75 °C) $\delta$ 0.20 (m, 2), 0.42 (m, 2), 0.89−0.96 (m, 1), 1.20−1.44 (m, 4), 1.36 (s, 9), 1.63 (s, 9), 1.60−1.81 (m, 2), 2.73−2.95 (m, 4), 3.03−3.26 (m, 4), 3.36−3.43 (m, 2), 3,84 (dd, 1, $J$ = 8.4, 5.3), 4.57 (m, 1), 6.32 (m, 1), 7.23 (t, 1, $J$ = 6.9), 7.31 (t, 1, $J$ = 6.9), 7.42 (s, 1), 6.60 (d, 1, $J$ = 6.9), 7.60 (d, 1, $J$ = 6.9), 8.02 (d, 1, $J$ = 8.1), 8.58 (d, 1, $J$ = 9.6). LRMS (MALDI-TOF) mass calcd for $C_{33}H_{49}N_4O_6S$ ($MH^+$) 629.3. Found 629.6. Anal. Calcd for $C_{33}H_{48}N_4O_6S$ C, 63.03; H, 7.69; N, 8.91. Found C, 63.19; H, 7.46; N, 8.71.

**Synthesis of the Focused Library of Somatostatin Mimetics**. To initiate library synthesis, the linker was coupled to large bead (40−60 mesh) aminomethyl resin and the support-bound thiol was generated as described previously. 2-Benzothiazolylyl 2-(4,4′-dimethoxytrityloxy)-ethyl disulfide (1.36 g, 2.50 mmol) dissolved in $CH_2Cl_2$ was then added to 5.0 g of the support-bound thiol in a 100-mL round-bottom flask and the reaction vessel stoppered under nitrogen and shaken for 21 h. An aliquot of resin was exposed to Ellman's reagent,[23] and no color change was observed, indicating that no free thiol remained in the solid support. The resin was collected by filtration and rinsed with DMF, $CH_2Cl_2$ (4×), and MeOH (2×), and dried in vacuo. The loading level of the resin at this stage was determined by quantitation of the 4,4′-dimethoxytrityl cation chromophore and found to be 0.19 ± 0.01 mequiv/g. The 4,4′-dimethoxytrityl ether was then cleaved by treatment of the resin with 3% trichloroacetic acid in $CH_2Cl_2$ (2 × 3 min) and then rinsed with $CH_2Cl_2$ (2×), MeOH, $CH_2Cl_2$ (2×), MeOH, and dried over $P_2O_5$. The resin was then solvated in 30 mL of $CH_2Cl_2$ and 1.05 mL (9.0 mmol) of 2,6-lutidine followed by 1.05 g (6.0 mmol) of mesyl anhydride were added while bubbling nitrogen through the 50-mL peptide flask. The flask was stoppered and shaken for 1 h. The resin was then rinsed with dry $CH_2Cl_2$ (4×), and the mesylation and rinsing steps were repeated. To cap any nonmesylated alcohol, the resin was solvated in 30 mL of $CH_2Cl_2$ and 1.57 mL (9.0 mmol) of *i*-$Pr_2EtN$ followed by 427 μL of acetyl chloride were added. After 5 min, the resin was rinsed with dry $CH_2Cl_2$ (4×) and dried in vacuo. Each of the 22 primary amines (2.0 mmol) were added to a sample vial and dissolved in 2 mL of anhydrous NMP. Resin (200 mg each) was then added to each vial and the vials immersed in a 50 °C oil bath for 12 h. The reaction solvent was filtered away, and the resin batches were rinsed with DMF (1 × 30 min) using a vacuum applied through a Teflon cannula to remove solvent. The resin was then allowed to solvate in 2.0 mL/vial of 3:2 dichloroethane/DMF to attain an isopicnic slurry. The resin was transferred as a slurry (210 μL/well) into the corresponding wells of modified 8 × 12 pipet tip trays (Labsystems, Finntip Universal, catalog No. 9400210). The pipet tip trays had been cut to fit into the wells of a microtiter plate. Three holes had been drilled (MC79 drill bit) in the bottom of each well to allow the passage of solvent while retaining the 40−60 mesh beads. After transfer, the resin beads were rinsed with DMF (1 × 10 min) and $CH_2Cl_2$ (3 × 10 min), allowed to air-dry for 1 h, and rinsed with dry DMF (1 × 15 min). The corresponding Fmoc amino acids ($i$ + 2 position) and α-bromo acids ($i$ + 1 position) were then coupled, and the resin was rinsed as described previously. A 300-mL mixture of 7:2:1 DMF/*i*-PrOH/$H_2O$ and 5% v/v *N*-methylmorpholine was purged with Ar (20 min), and 7.5 mL of a 1.0 M solution of triethylphosphine in THF was added. Each well of the two microtiter plates was treated with 750 μL of the solution, and the beads were immersed in the microtiter plates. An additional 400 μL of the cleavage solution was added through the top of the modified pipet tip holders containing the resin beads. The microtiter plate assemblies were placed in an oven under a nitrogen atmosphere and heated to 40−45 °C for 16 h and then to 60 °C for 3.5 h. The modified pipet tip holders were elevated above the microtiter plates in such a way that the solvent could drip into the microtiter wells below for 10 min. Cleavage solvent was removed by concentration in vacuo on a Jouan RC10 concentrator equipped with a microtiter-plate rotor. Methanol (1 mL) was then added to each well, and the resulting solutions were reconcentrated in vacuo. The side-chain protecting groups were removed by addition of 0.4 mL of 18:1:1 TFA/dimethyl

(36) Milligen Technical Note 3.10.

sulfide/water to each well via Drummond manifold. After 0.5 h, the cleavage solutions were reconcentrated in vacuo. DMSO (100 μL) was added to each well, and the plates were stored at −20 °C. Some triethyl phosphine oxide byproduct contaminated the wells of the resultant library, but verification of the active wells with purified material revealed that the contaminant had little or no effect on binding activity in this competitive radioligand binding assay.

Seven compounds from each microtiter plate were picked at random and analyzed by mass spectrometry in a matrix of α-cyano-4-hydroxycinnamic acid on a Perspective Biosystems MALDI-TOF instrument. Of the Fourteen 14 samples, 13 showed the proper molecular ion.

**Synthesis of β-turn Mimetics for Validation of Bioactivity**. Five of the most potent compounds from the directed library and three alanine scan compounds were synthesized on a multimilligram scale as described previously. These compounds were purified by silica column chromatography and characterized by $^1$H NMR and low resolution mass spectrometry MALDI-TOF or FAB. The characterization data are listed below after the appropriate compound code.

**(1h):** $^1$H NMR (500 MHz, DMSO-$d_6$, 75 °C) δ 1.20−1.45 (m, 3H), 1.60−1.70 (m, 2H), 1.92 (m, 1H), 2.62−3.60 (m, 5H), 3.98 (m, 1H), 4.11−4.21 (m, 2H), 4.61 (m, 1H), 4.79 (m, 1H), 5.38 (m, 1H), 5.68 (d, $J$ = 15.6 Hz, 1H), 6.97−7.19 (m, 3H), 7.30−7.59 (m, 6H), 7.84 (d, $J$ = 8.8, 1H), 7.92 (m, 1H), 8.06 (m, 1H), 8.29 (m, 1H), 10.60 (m, 1H). LRMS (MALDI-TOF) α-cyano-4-hydroxycinnamic acid matrix: mass calcd for $C_{30}H_{35}N_4O_2S$ (MH+) 515.2, found 515.3.

**(1i):** $^1$H NMR (500 MHz, DMSO-$d_6$, 75 °C) δ 1.20−1.45 (m, 3H), 1.60−1.70 (m, 2H), 1.92 (m, 1H), 2.62−3.60 (m, 5H), 3.98 (m, 1H), 4.11−4.21 (m, 2H), 4.61 (m, 1H), 4.79 (m, 1H), 5.38 (m, 1H), 5.68 (d, $J$ = 15.6 Hz, 1H), 6.97−7.19 (m, 3H), 7.30−7.59 (m, 6H), 7.84 (d, $J$ = 8.8, 1H), 7.92 (m, 1H), 8.06 (m, 1H), 8.29 (m, 1H), 10.60 (m, 1H). LRMS (MALDI-TOF) α-cyano-4-hydroxycinnamic acid matrix mass calcd for $C_{30}H_{35}N_4O_2S$ (MH+) 515.2, found 515.6.

**(1j):** $^1$H NMR (500 MHz, DMSO-$d_6$, 75 °C) δ 1.32 (q, $J$ = 7.5 Hz, 1H), 1.47 (m, 1H), 1.57−1.69 (m, 2H), 1.92 (m, 1H), 2.75 (m, 3H), 2.83 (m, 2H), 3.00−3.10 (m, 1H), 3.25 (d, $J$ = 14.6, 8.9 Hz, 1H), 3.37 (m, 1H), 3.78 (dd, $J$ = 8.9,5.3 Hz, 1H), 4.67 (d, $J$ = 8.0, 1H), 4.73 (m, 1H), 5.22 (d, $J$ = 15.4, 1H), 6.96 (t, $J$ = 7.5, 1H), 7.06 (m, 2H), 7.32 (d, $J$ = 8.0, 1H), 7.38 (d, $J$ = 6.9 Hz, 1H), 7.45 (t, $J$ = 8.0 Hz, 1H), 7.50−7.54 (m, 3H), 7.85 (d, $J$ = 8.0 Hz, 1H), 7.93 (m, 1H), 8.03 (m, 1H), 8.62 (d, $J$ = 9.7, 1H), 10.64 (s, 1H). LRMS (MALDI-TOF) α-cyano-4-hydroxycinnamic acid matrix mass calcd for $C_{30}H_{35}N_4O_2S$ (MH+) 515.2, found 515.4.

**(1k):** $^1$H NMR (500 MHz, DMSO-$d_6$, 75 °C) δ 1.16−1.26 (m, 2H), 1.49−1.59 (m, 3H), 1.83 (m, 1H), 2.60−2.80 (m, 4H), 2.95−3.46 (m, 3H), 3.60 (m, 2H), 3.75 (m, 1H), 3.91 (m, 1H), 4.30 (m, 1H), 4.46 (m, 1H), 4.65 (m, 1H), 6.97 (t, $J$ = 7.5, 1H), 7.06 (t, $J$ = 7.5 Hz, 1H), 7.14 (m, 1H), 7.19 (m, 1H), 7.33 (m, 2H), 7.40 (m, 2H), 7.50−7.57 (m, 2H), 8.17 (m, 1H), 10.63 (s, 1H). HRMS (FAB) exact mass calcd for $C_{27}H_{35}N_4O_4S_2$ ($MH^+$) 511.2201, found 511.2202.

**(1l):** $^1$H NMR (500 MHz, DMSO-$d_6$, 75 °C) δ 1.10−1.60 (m, 5H), 1.90 (m, 1H), 2.62−4.21 (m, 10H), 4.53 (m, 1H), 4.75 (m, 1H), 5.95 (s, 2H), 6.72−6.87 (m, 3H), 6.97−7.19 (m, 3H), 7.32 (m, 1H), 7.55 (m, 1H), 8.21 (m, 1H), 10.65 (m, 1H). LRMS (MALDI-TOF) α-cyano-4-hydroxycinnamic acid matrix mass calcd for $C_{27}H_{33}N_4O_4S$ (MH+) 509.2, found 509.6.

**(1m):** $^1$H NMR (300 MHz, MeOH-$d_4$, 55 °C) δ 1.22−1.29 (m, 4H), 1.41−1.52 (m, 2H), 2.22−2.37 (m, 2H), 2.72−2.79 (m, 3H), 2.89−2.93 (m, 1H), 3.18−3.21 (M, 1H), 3.30−3.34 (m, 2H), 3.51−3.59 (m, 2H), 4.61−4.72 (m, 2H), 7.21−7.39 (m, 2H), 7.50 (s, 1H), 7.57−7.59 (m, 1H), 7.71−7.76 (m, 1H). HRMS (FAB) exact mass calcd for $C_{20}H_{28}N_4O_2S$ ($MH^+$) 389.2009, found 389.2004.

**(1n):** $^1$H NMR (300 MHz, MeOH-$d_4$, 55 °C) δ 1.35 (d, $J$ = 6.5, 3H), 2.41−2.45 (m, 1H), 2.62−2.74 (m, 1H), 3.07−3.09 (m, 2H), 3.31−3.42 (m, 2H), 3.92−3.95 (m, 1H), 4.13 (d, $J$ = 13.0, 1H), 4.91−4.95 (m, 1H), 5.68−5.73 (d, $J$ = 13.0, 1H), 7.18−7.22 (m, 3H), 7.25 (d, $J$ = 7.3, 1H), 7.38 (d, $J$ = 6.1, 2H), 7.49−7.47 (m, 2H), 7.63 (d, $J$ = 7.3, 1H), 7.78−7.84 (m, 2H), 8.04 (d, $J$ = 7.7, 1H). HRMS (FAB) exact mass calcd for $C_{27}H_{27}N_3O_2S$ ($MH^+$) 558.2413, found 558.2415.

**(1o):** $^1$H NMR (300 MHz, DMSO-$d_6$, 75 °C) δ 1.18−1.22 (m, 1H), 1.29 (m, 3H), 1.41−1.49 (m, 2H), 1.51−1.67 (m, 2H), 2.58−2.62 (m, 2H), 2.73−2.68 (m, 1H), 2.91−2.97 (m, 2H), 3.04−3.13 (m, 1H), 3.49−3.56 (m, 1H), 3.83−3.87 (m, 1H), 4.0 (d, $J$ = 14.4, 1H), 4.69−4.76 (m, 1H), 5.75 (d, $J$ = 14.5, 1H), 7.41−7.59 (m, 3H), 7.62−7.71 (m, 2H), 7.80−7.83 (m, 1H), 7.91−7.98 (m, 1H). HRMS (FAB) exact mass calcd for $C_{22}H_{29}N_3O_2S$ ($MH^+$) 400.2045, found 400.2050.

**Procedure for Radioligand Binding Assay**. Cell membranes (2−30 μg protein) were incubated with 0.03 nM [$^{125}$I]-[Tyr$^{11}$]-SRIF and increasing concentrations of SRIF or SRIF analogues for 90 min at room temperature.[37] Nonspecific binding was defined with 1 μM SRIF. The assay was terminated by rapid filtration through Whatman GF/C glass fiber filters soaked in 0.5% polyethylenimine (PEI), followed by 3 × 3 mL washes of 50 mM Tris-HCl pH 7.4 containing 5 mg/mL bovine serum albumin (BSA). Radioactivity in the filters was determined using a Canberra Packard Cobra II Auto-counter. Data were analyzed by nonlinear regression using the curve-fitting programs EBDA[38] and LIGAND.[39]

**Acknowledgment.** This work was supported by funding from the National Institutes of Health (GM53696). Å.R. would like to thank the Knut and Alice Wallenberg Foundation for funding.

JA983742P

(37) Castro, S. W.; Buell, G.; Feniuk, W.; Humphrey, P. P. A. *Br. J. Pharmacol.* **1996**, *117*, 639−646.
(38) Mcpherson, G. A. *J. Pharmacol. Methods* **1985**, *14*, 213−228.
(39) Munson, P. J.; Rodbard, D. *Anal. Biochem.* **1980**, *107*, 220−239.